Peptidylarginine Deiminase Inhibitor Cl-amidine Attenuates Cornification and Interferes with the Regulation of Autophagy in Reconstructed Human Epidermis

Laura Cau, Hidenari Takahara, Paul R Thompson, Guy Serre, Marie-Claire Méchin, Michel Simon

SUPPLEMENTARY MATERIALS AND METHODS

Recombinant proteins

Purified recombinant human peptidylarginine deiminases PAD1-3 (active forms without any tag) and poly-histidine tagged purified recombinant filaggrin (FLG-His) were produced and purified as previously described (Kanno et al., 2000; Guerrin et al., 2003; Méchin et al., 2005).

In vitro evaluation of Cl-amidine efficacy

To assess the efficacy of Cl-amidine against epidermal PADs, *in vitro* PAD activity assays were performed as previously described (Méchin et al., 2005; Méchin et al., 2010) in the presence of various concentrations of Cl-amidine (0-100 µM). Recombinant PAD1, PAD2 or PAD3 (40 milliunits/assay) were pre-incubated with Cl-amidine in 100 mM Tris-HCl pH 7.4, 10 mM $CaCl_2$, 5 mM DTT at 37°C for 10 min.

Then, FLG-His (100 ng/assay) was added as a substrate and the mix was incubated at 37°C for 1 hour for PAD1 and PAD3 and for 20 min for PAD2. The reactions were stopped by the addition of Laemmli buffer (175 mM Tris-HCl, pH 6.8, 7.5% SDS, 25% glycerol, 12.5% β-mercaptoethanol) and boiling for 3 min. Samples were analyzed by western blotting with the AMC antibodies as described below.

Light microscopy and immunohistology

RHE samples were fixed in 4% formaldehyde containing buffer (Sigma-Aldrich, St Louis, MO) for 24 hours at 4°C, and subsequently paraffin-embedded. For light microscopy analyses, five-micron sections were stained with hematoxylin and eosin. For indirect immunofluorescence analyses, after deparaffinization, rehydration and incubation in a blocking solution (2% bovine serum albumin and 0.05% Tween-20 in PBS), sections were first incubated with primary antibodies and then with the appropriate Alexa Fluor conjugated secondary antibody (Alexa Fluor 555 anti-rabbit IgG and Alexa Fluor 488 anti-mouse IgG, Invitrogen Life Technologies, Carlsbad, CA) diluted to 1/1000 and 4'-6-diamidino-2-phenylindole (DAPI, Sigma-Aldrich) diluted to 1 µg/ml. Slides were mounted in Mowiol 4-88 (Calbiochem, San Diego, CA) and

observed under a Nikon Eclipse 80i fluorescence microscope equipped with a Nikon DXM 1200C digital camera and NIS image analysis software (Nikon, Tokyo, Japan).

Western blot analysis

RHE specimens were lyzed by boiling in Laemmli buffer. In some cases, detergent soluble proteins were extracted in the presence of Nonidet P-40, as previously described (Nachat et al., 2005). Epidermal proteins were resolved by SDS - 10% polyacrylamide gel electrophoresis (SDS-PAGE) and electrotransferred onto nitrocellulose membranes (GE Healthcare, Danderyd, SE). Membranes were blocked in a Tris-HCl buffer containing 0.05% Tween-20 and 5% skim milk (for detection with AMC, anti-actin and anti-sestrin-2 antibodies) or 5% bovine serum albumin (for detection with anti-LC3 antibody), then incubated overnight at 4°C with primary antibodies and finally incubated for 2 hours at room temperature with secondary horseradish peroxidase-conjugated antibodies diluted to 1:10000 (Goat Anti-Rabbit IgG-HRP, SouthernBiotech, Birmingham, AL; Goat Anti-Mouse IgG-HRP, Bethyl Laboratories, Montgomery, TX). The detection was realized with ECL Prime system (GE Healthcare) and images were acquired with a G:BOX Chemi XT4 CCD camera

(Syngene, Cambridge, United Kingdom) and GeneSys software (Genesys, Daly City, CA). ImageJ software was used to quantify immunoreactive bands. Signals were normalized to Ponceau red staining for deiminated proteins (detected with the AMC antibodies) and to actin immunodetection for LC3, sestrin-2 and p62.

Cell viability assay

Cell viability of RHEs was determined using an MTT (3-(4,5-dimethylthiazol-2-yl)-2,5-diphenyl tetrazolium bromide; Sigma-Aldrich) reduction assay as described previously (Pendaries et al., 2014; Frankart et al., 2012). RHEs topically treated with 3% SDS were used as a control. Optical density was measured at 550 nm.

SUPPLEMENTARY COMMENTARY ABOUT CL-AMIDINE CONCENTRATIONS

RHEs were treated with a higher concentration of Cl-amidine (800 µM) than the concentration effective against recombinant PADs in vitro. This could be surprising. In fact, we have no idea of the intracellular concentration of the drug; it could be much less than in the culture medium. In addition, 800 µM (0,339 mg/ml) is in the same range as the theoretical fluid concentration *in vivo* in mice effectively treated with Cl-amidine.

Indeed, in collagen-induced arthritis, mice were IP injected daily during 35 days with 0.2-1 mg (Willis et al., 2011). In experimental colitis model, mice were IP treated daily during 7 days with 1.5 mg (Chumanevich et al., 2011).

SUPPLEMENTARY REFERENCES

Agarwal S, Bell CM, Taylor SM, Moran RG. p53 Deletion or Hotspot Mutations Enhance mTORC1 Activity by Altering Lysosomal Dynamics of TSC2 and Rheb. Mol Cancer Res. 2016; 14: 66-77.

Cau L, Pendaries V, Lhuillier E, Thompson PR, Serre G, Takahara H, et al. Lowering relative humidity level increases epidermal protein deimination and drives human filaggrin breakdown. J Dermatol Sci 2017; 86:106-13.

Chumanevich AA, Causey CP, Knuckley BA, Jones JE, Poudyal D, Chumanevich AP, Davis T, Matesic LE, Thompson PR, Hofseth LJ. Suppression of colitis in mice by Cl-amidine: a novel peptidylarginine deiminase inhibitor. Am J Physiol Gastrointest Liver Physiol 2011; 300: G929–G938.

Frankart A, Malaisse J, De Vuyst E, Minner F, de Rouvroit CL, Poumay Y. Epidermal morphogenesis during progressive in vitro 3D reconstruction at the air-liquid interface. Exp Dermatol. 2012; 21: 871-5.

Guerrin M, Ishigami A, Méchin M-C, Nachat R, Valmary S, Sebbag M et al. cDNA cloning, gene organization and expression analysis of human peptidylarginine deiminase type I. Biochem J 2003; 370: 167-74.

Jones JE, Slack JL, Fang P, Zhang X, Subramanian V, Causey CP, et al. Synthesis and screening of a haloacetamidine containing library to identifiy PAD4 selective inhibitors. ACS Chem Biol 2012; 7:160-5.

Kanno T, Shiraiwa M, Takahara H, Kawada A, Tezuka T, Yamanouchi J, et al. Human Peptidylarginine Deiminase Type III: Molecular Cloning and Nucleotide Sequence of the cDNA, Properties of the Recombinant Enzyme, and Immunohistochemical Localization in Human Skin. J Invest Dermatol 2000; 115: 813-23.

Méchin M-C, Enji M, Nachat R, Chavanas S, Charveron M, Ishida-Yamamoto A, et al. The peptidylarginine deiminases expressed in human epidermis differ in their substrate specificities and subcellular locations. Cell Mol Life Sci 2005; 62: 1984-95.

Méchin M-C, Coudane F, Adoue V, Arnaud J, Duplan H, Charveron M, et al. Deimination is regulated at multiple levels including auto-deimination of peptidylarginine deiminases. Cell Mol Life Sci. 2010; 67: 1491-503.

Nachat R, Méchin M-C, Takahara H, Chavanas S, Charveron M, Serre G, et al. Peptidylarginine Deiminase Isoforms 1–3 Are Expressed in the Epidermis and Involved in the Deimination of K1 and Filaggrin. J Invest Dermatol 2005; 124: 384-93.

Pendaries V, Malaisse J, Pellerin L, Le Lamer M, Nachat R, Kezic S, et al. Knockdown of Filaggrin in a Three-Dimensional Reconstructed Human Epidermis Impairs Keratinocyte Differentiation. J Invest Dermatol 2014; 134: 2938-46.

Scherz-Shouval R, Weidberg H, Gonen C, Wilder S, Elazar Z, Oren M. p53-dependent regulation of autophagy protein LC3 supports cancer cell survival under prolonged starvation. Proc Natl Acad Sci 2010; 107: 18511-6.

Tarcsa E, Marekov LN, Mei G, Melino G, Lee S-C, et al. Protein Unfolding by Peptidylarginine Deiminase. SUBSTRATE SPECIFICITY AND STRUCTURAL RELATIONSHIPS OF THE NATURAL SUBSTRATES TRICHOHYALIN AND FILAGGRIN. J Biol Chem 1996; 271: 30709-16.

Wang S, Chen X-A, Hu J, Jiang J-K, Li Y, Chan-Salis KY, et al. ATF4 Gene Network Mediates Cellular Response to the Anticancer PAD Inhibitor YW3-56 in Triple-Negative Breast Cancer Cells. Mol Cancer Ther. 2015; 14: 877-88.

Willis VC, Gizinski AM, Banda NK, Causey CP, Knuckley B, Cordova KN, Luo Y, Levitt B, Glogowska M, Chandra P, Kulik L, Robinson WH, Arend WP, Thompson PR, Holers VM. J Immunol 2011; 186:4396-404.

LEGENDS OF SUPPLEMENTARY FIGURES

Figure S1. ***In*** **vitro inhibition of the activity of epidermal petidylarginine deiminases (PADs) using Cl-amidine.** Purified recombinant histidine-tagged filaggrin (FLG-His; 100 ng/assay) was incubated at 37°C with recombinant PAD1, PAD2 or PAD3, and Cl-amidine at

different concentrations (0-100 μM). The reaction products were then analyzed by western blotting with an antibody directed to modified citrullines (AMC). The arrow head indicates the concentration of Cl-amidine from which an inhibitory effect on FLG deimination is clearly observed. Molecular mass markers are indicated in kDa on the left of each blot. Note that deimination induces a progressive increase in the apparent molecular mass of FLG, from 40 kDa (when not deiminated) up to around 75 kDa for the totally deiminated form, as previously observed (Tarsca et al., 1996; Méchin et al., 2005; Nachat et al., 2005; Méchin et al., 2010). A clear decrease in filaggrin deimination was observed from Cl-amidine concentrations of 3.125, 50 and 25 μM for PAD1, PAD2 and PAD3, respectively. This showed that Cl-amidine was more specific for PAD1 than for PAD2 and PAD3 but was nevertheless able to inhibit the activity of the three isotypes. This substantiates previously published data showing inhibition of the same PADs with similar efficacy using benzoyl-L-arginine ethyl ester as a synthetic substrate (Jones et al., 2012).

Figure S2. Deimination rate and peptidylarginine deiminase (PAD1 and PAD3) expression in reconstructed human epidermis (RHEs). (**a**) Normal human skin and RHEs harvested after 6, 8, 10 and 12 days of culture at the air-liquid interface (D6-D12) were stained with hematoxylin-eosin (H&E) and immunodetected with the AMC antibody. (**b**) Total protein extracts were immunodetected with AMC and anti-actin antibodies. Molecular mass markers are indicated in kDa. (**c**) The *PADI1* and *PADI3* mRNA levels were quantified by qPCR using *YWHAZ* as reference for normalization and expressed relative to the amount on D4, arbitrarily set to 100%. (**d**) RHEs were immunodetected with antibodies specific for PAD1 and PAD3, as indicated. Nuclei (blue) are stained with 4′,6-diamidino-2-phenylindole. The polycarbonate filter and dermo-epidermal junctions are indicated by white dashed lines. Scale bars = 25 μm. NHE, normal interfollicular human epidermis.

Figure S3. Immunofluorescence double labelling of LC3 and either PAD1 or PAD3 in RHEs. Sections of fixed untreated RHEs were analyzed, after antigen retrieval buffer incubation, by indirect immunofluorescence with antibodies directed against PAD1 and LC3 (**a**) or PAD3 and LC3 (**b**). Sections were observed with an SP8 confocal microscope (x63). The illustrations correspond to the sum of fluorescence intensities of all acquired consecutive images (z-stacks). Nuclei are counterstained with 4′,6-diamidino-2-phenylindole (Dapi). Scale bars = 25 μm.

Figure S4. Partial co-localization of PADs with LC3. Untreated RHEs sections were analyzed by confocal microscopy after double labelling with anti-LC3 and either anti-PAD1 or anti-PAD3 antibodies, as indicated. The image superposition of PAD1/LC3 and PAD3/LC3 are shown on the right panels (Merge). The spectral profiles of each fluorochrome (Alexa Fluor 488 (green) for PADs, and Alexa Fluor 555 (red) for LC3) are recorded along the white lines shown in the merge images and depicted as RGB profilers. Scale bar = 25 μm.

SUPPLEMENTARY TABLES

Table S1. Thresholded Manders coefficients

Antigens	Condition	Manders coefficients
PAD1/LC3	Control	A (green): 0.2236 B (red): 0.1849
PAD3/LC3	Control	A (green): 0.1740 B (red): 0.1471

PAD1- and PAD3-specific polyclonal antibodies were detected using Alexa Fluor 555-labeled secondary antibodies (green channel) whereas LC3-specific monoclonal antibody was detected using Alexa Fluor 488-labeled secondary antibodies (red channel). Manders' coefficients A and B were calculated through Imaris software. They refer to green and red channels, respectively.

Table S2. Antibodies

Antigen	Antibody	Source (Reference)	Dilution
PAD1	pAb[$]	Sigma-Aldrich-Merck, Paris, France (HPA062294)	1/100 (IF)
PAD3	pAb	AbCam, Paris, France (Ab50246)	1/100 (IF)
LC3*	mAb	Neobiotech, Nanterre, France (Clone 9H5; NB-22-7745)	1/200 (IF)
LC3*	pAb	Cell Signaling Technology, Danvers, MA (2775)	1/1000 (WB)
p62/SQSTM1	pAb	Proteintech, Manchester, UK (18420-1-AP)	1/1000 (WB)
Sestrin2	pAb	Proteintech (10795-1-AP)	1/1000 (WB)

[$]pAb, polyclonal antisera; mAb, monoclonal antibody; *for LC3 staining, epitope retrieval incubation was performed in a 50 mM glycine-HCl buffer pH 3.5 at 95°C.

Table S3. List of primers

Gene	*Sens*	*Sequence*	References
ATG5	F	GCAGATGGACAGTTGCACACA	Scherz-Shouval et al., 2010
	R	TTTCCCCATCTTCAGGATCAA	
SESN2	F	ACAAGTGTTGTGGCCTTCCTGAAC	Agarwal Stuti et al., 2016
	R	ATGGGTGAATGGCAAGTAGGAGGT	

MAP1LC3B	F	ACCATGCCGTCGGAGAAG	Scherz-Shouval et al., 2010
	R	ATCGTTCTATTATCACCGGGATTTT	
ATF4	F	CAGCAAGGAGGATGCCTTCT	Wang et al., 2015
	R	TCCTTCAAATCCATTTTCTCCAA	
YWHAZ	F	ACTTTTGGTACATTGTGGCTTCAA	Méchin et al., 2010
	R	CCGCCAGGACAAACCAGTAT	Cau et al., 2017

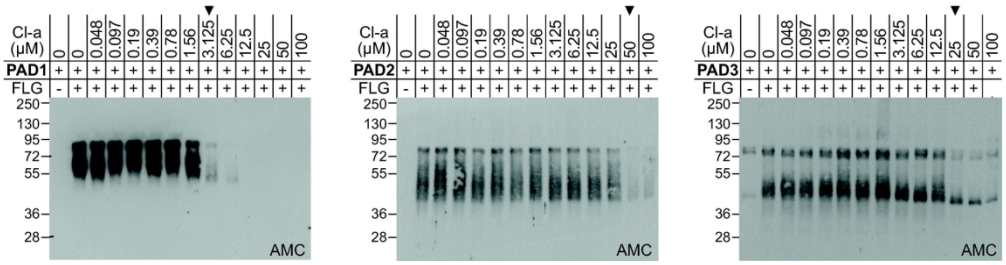

175x44mm (300 x 300 DPI)

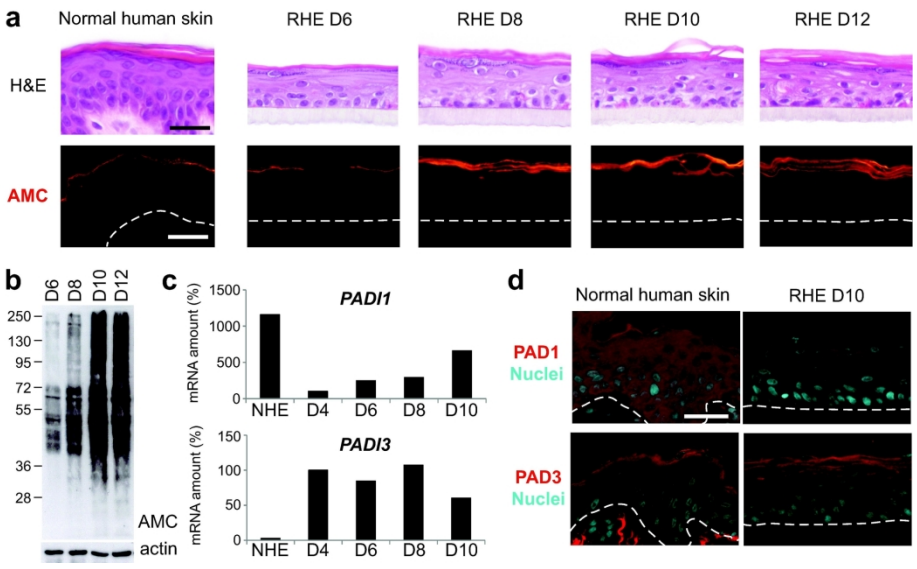

196x110mm (300 x 300 DPI)

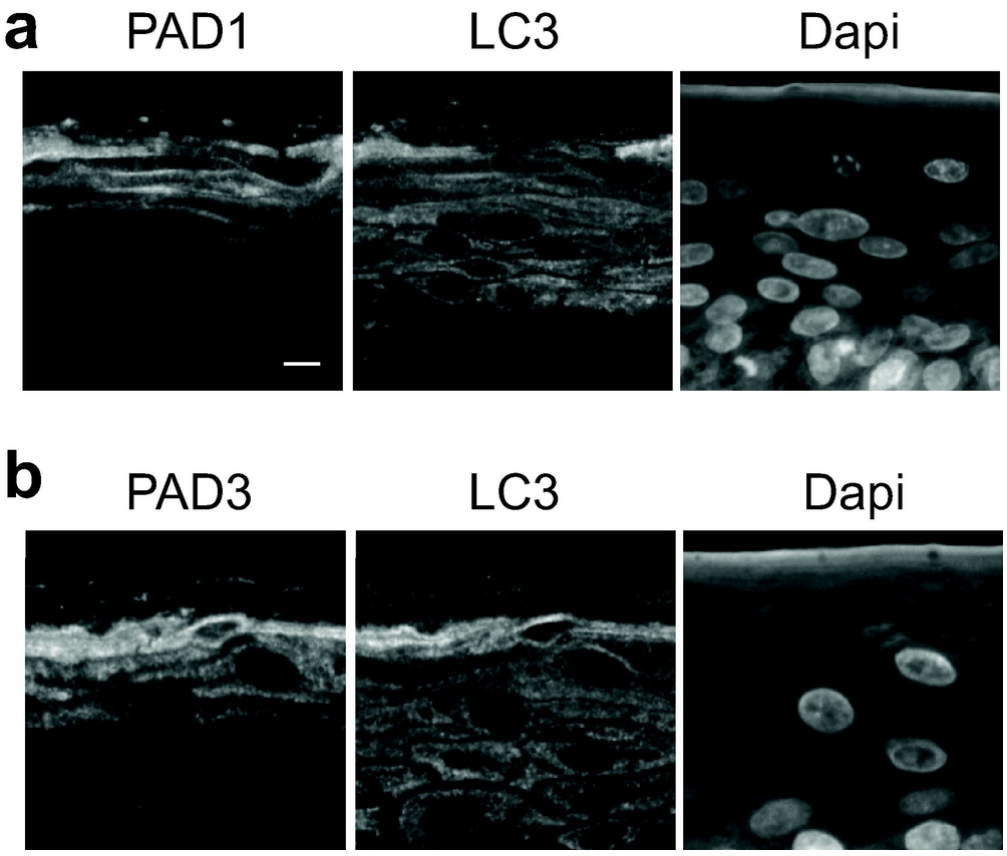

84x72mm (300 x 300 DPI)

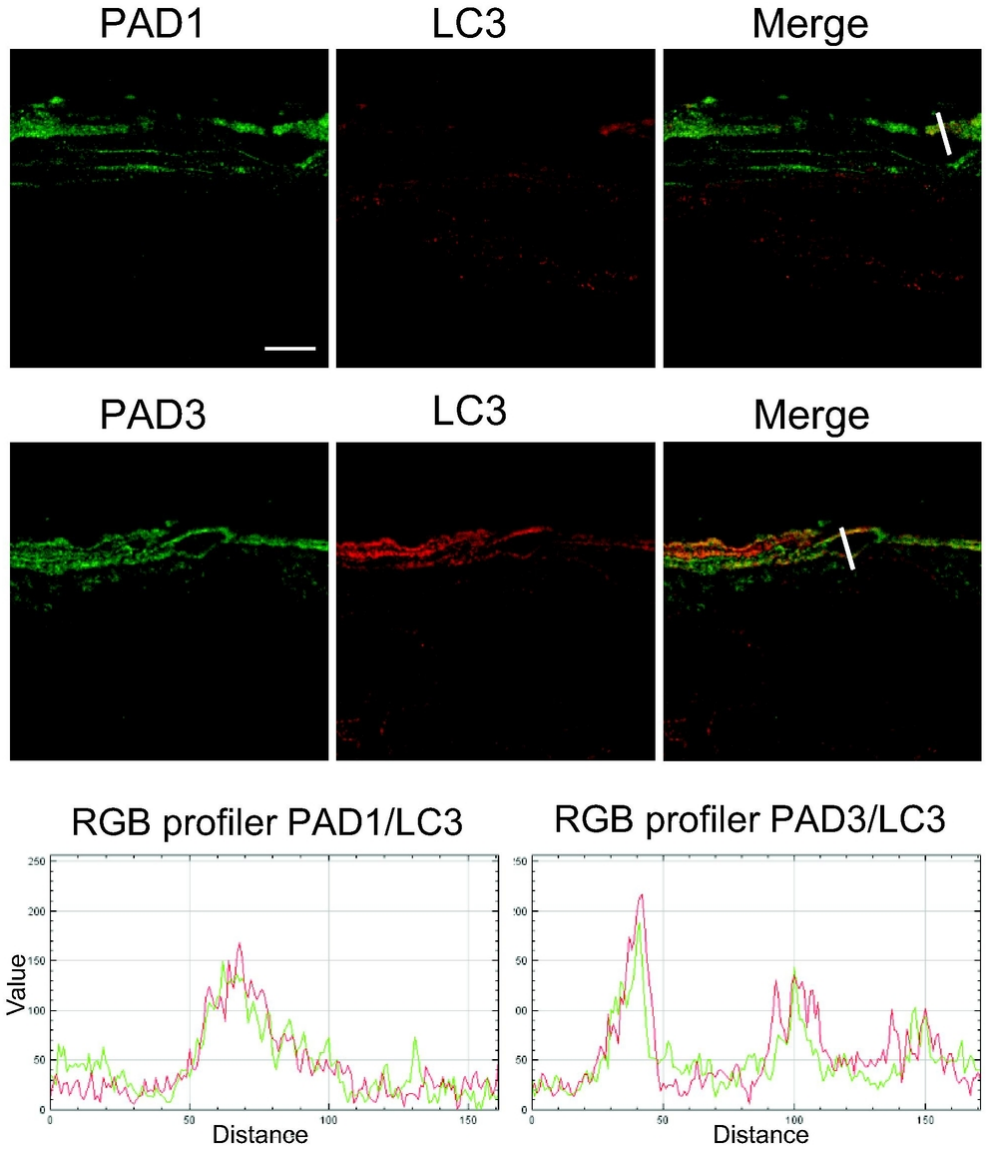

84x97mm (300 x 300 DPI)